RSC Advances

PAPER

View Article Online
View Journal | View Issue

Cite this: *RSC Adv.*, 2019, **9**, 20528

Synthesis and catalytic performance of a small crystal NaY zeolite with high SiO_2/Al_2O_3 ratio

Liang Mu, WeiWei Feng, Haobin Zhang, Xiubin Hu and Qingyan Cui *

Received 4th May 2019
Accepted 24th June 2019

DOI: 10.1039/c9ra03324f

rsc.li/rsc-advances

A small crystal NaY zeolite with a high SiO_2/Al_2O_3 ratio was successfully synthesized with seeding and without organic template, and the effects of the silicon source, aging time and Na_2O seeding content on the crystal size of NaY zeolite were investigated. The synthesized samples were characterized by X-ray diffraction (XRD), scanning electron microscopy (SEM), Fourier-Transform Infrared (FT-IR) spectroscopy and N_2 adsorption–desorption. The results showed that the silicon source used to prepare seeding had a great effect on the crystal size of NaY zeolite, NaY zeolite with average size of 100 nm and SiO_2/Al_2O_3 ratio of 5.42 was obtained by using the seeding prepared with silica sol. Moreover, the crystal size of NaY zeolite decreased with an extension of the aging time and an increase of the Na_2O content of seeding. The catalytic performance of small crystal Y zeolite was evaluated in the hydrocracking of vacuum gas oil (VGO), the catalyst with smaller crystal Y zeolite presented higher VGO conversion and middle distillates selectivity than those with larger ones due to its higher surface area and more amount of mesoporous.

1 Introduction

Zeolites are comprised of silicon and aluminum oxide tetrahedrons (SiO_4 and AlO_4^-) through oxygen atom linking to form a three-dimensional network structure, in which a porous framework with micropores in the range of 2–10 Å are present. Zeolites have high surface area due to their micropores structure and exhibit acidic property depending on their compositions. Y zeolite is a kind of faujasite type zeolites with a SiO_2/Al_2O_3 ratio larger than 3, its basic structure units, the sodalite cages, are assembled to form a spherical supercage up to 1.2 nm in the diameter, and the large cavity is 12-membered oxygen ring with a diameter of 7.1–7.3 Å.[1,2] Y zeolite is widely employed as catalyst in the fluid catalytic cracking (FCC) and hydrocracking for conversion of petroleum into fuel oil based on its large amount of acid sites, thermal stability and so on.[3–7]

Crystal size of zeolite is closely related to its properties, which have an important impact on the application. Reduction of crystal size can increase the ratio of external to internal number of atoms, thus the smaller zeolite crystals exhibit larger surface area and larger amount of activity sites. Additionally, smaller zeolite crystals with short pore channels are beneficial to the diffusion of reactant and intermediate product.[8–10] Thus, small crystal zeolite used as catalyst has attracted much attention due to its high cracking activity, well catalytic selectivity and superior resistibility to coke deposition.[11–14]

Small crystal NaY zeolite was successfully synthesized with the assistance of organic templates, such as tetramethylammonium bromide (TMABr), tetramethylammonium hydroxide (TMAOH) and crown ether family organic, by optimizing the type and amount of organic template, composition of initial precursor suspensions and synthesis conditions.[15–18] However, the usage of organic template in small crystal zeolite synthesis has several drawbacks, for instance, organic templates are expensive and non-recyclable, as well as the removal of organic templates by calcination leads to an aggregation of small crystals in large particles and the environmental pollution due to the poisonous gas emissions, in addition, the usage of organic template may result into the low yield of small crystal zeolite.[11,19–21] Therefore, an approach without organics as structure directing agent is significant to synthesize small crystal Y zeolite.

There are some reports about the synthesis of small crystal Y zeolite without organic template. Mintova *et al.* has successfully synthesized nanosized Y zeolite with SiO_2/Al_2O_3 ratio of 4.2 *via* controlling an uniform nucleation during the gel preparation.[22] Zhang *et al.* reported that NaY zeolite with the crystal size below 400 nm was synthesized using a two-stage variable-temperature program.[23] Daou *et al.* has synthesized zeolite Y with the crystal sizes below 30 nm and SiO_2/Al_2O_3 about 4.4 by progressive adding of a silica source during synthesis combined with the use of prolonged aging time.[24] Alhassan *et al.* found that nanosized zeolite Y can be synthesized in the presence of alkali metal chloride salt.[25] Reinoso *et al.* reported that nanocrystalline NaY zeolite was synthesized at low temperature *via* applying ultra-assisted aging.[26] Cardoso *et al.* synthesized nanosized

College of Chemical Engineering, Fuzhou University, Fuzhou, China. E-mail: qycui@163.com; Tel: +86-188-6011-8629

faujasite crystals with the SiO_2/Al_2O_3 ratio of 3.0 through a simple synthesis procedure.[27] However, the synthesized small crystal Y zeolite had low SiO_2/Al_2O_3 ratio as reported in the literature. It is well known that the physicochemical properties of zeolites are mainly dependent on the framework SiO_2/Al_2O_3 ratio, and an increase of the SiO_2/Al_2O_3 ratio in Y zeolite framework can improve its hydrothermal stability, which is beneficial to its catalytic performance.[28–31] Therefore, the development of small crystal and high SiO_2/Al_2O_3 ratio (larger than 5.0) Y zeolite synthesis is important, but there is few report about synthesis of small crystal and high SiO_2/Al_2O_3 ratio Y zeolite in the absence of organic template.[28]

Seeding, acted as structure directing agent, plays an important role in the zeolite synthesis process, which has been studied. Seeding can promote zeolite nucleation and growth as well as induce the initial synthesis gel to produce target phase rather than other phases, it is in favour of improving the purity of crystal product and expanding the range of gel composition.[32–35] Seeding also can decrease the crystal size and change the elemental composition of zeolite.[36,37] Thompson *et al.* studied the effect of seeding on the zeolite synthesis, and found that seeding added into zeolite synthesis system can provide more cumulative surface area for assimilation of nutrient material from solution, thus crystallization process was accelerated with increasing amounts of seeding surface area.[38] Bronic *et al.* reported that nuclei were produced immediately in the presence of seeding in the zeolite synthesis system on the basis of the secondary nucleation mechanism.[39] However, the effects of preparation conditions of seeding on the crystals size and SiO_2/Al_2O_3 ratio of Y zeolite have not been reported.

In this study, small crystal and high SiO_2/Al_2O_3 ratio Y zeolite in the absence of organic template was synthesized, and the effects of preparation conditions of seeding (silicon source, aging time and Na_2O content) on the crystal size and SiO_2/Al_2O_3 ratio in Y zeolite were investigated. In addition, the catalytic performance of synthesized Y zeolite was evaluated in the hydrocracking of vacuum gas oil (VGO).

2 Experimental

2.1 NaY zeolite synthesis

NaY zeolite was synthesized in the absence of organic template *via* the hydrothermal method. Firstly, the seeding gel was prepared by mixing sodium aluminum (Guangfu Fine Chemical Co. Ltd.), sodium hydroxide (Beijing Modern Oriental Fine Chemical Co. Ltd.), silica sol (40 wt% SiO_2 and 60 wt% H_2O, Beijing Modern Oriental Fine Chemical Co. Ltd.) or sodium silicon (28 wt% SiO_2, 9.1 wt% Na_2O and 62.9 wt% H_2O, Beijing Modern Oriental Fine Chemical Co. Ltd.) and deionized water with vigorous stirring for 1 h, and then aged at 30 °C for different time to obtain the seeding. The molar composition of seeding gel was $12–18Na_2O : 1Al_2O_3 : 18SiO_2 : 320H_2O$.

The molar composition of initial precursor gel for synthesized NaY zeolite was $5Na_2O : 1\ Al_2O_3 : 14.5SiO_2 : 300H_2O$. The sodium silicon, sodium aluminum, sodium hydroxide, aluminum sulfate (Beijing Modern Oriental Fine Chemical Co. Ltd.), deionized water and prepared seeding were mixed with vigorous stirring at 0 °C for 1 h, and then the precursor gel was transferred in Teflon autoclave, aged at 30 °C and hydrothermally crystallized at 95 °C. Finally, the solid sample was obtained by filtrating, washing and drying at 120 °C for 6 h.

2.2 Catalysts preparation

The synthesized NaY zeolite was ion-exchanged with 1.0 M NH_4NO_3 (Beijing Modern Oriental Fine Chemical Co. Ltd.) aqueous solution at 95 °C for 3 h, and then dried at 120 °C for 6 h and calcined at 500 °C for 4 h. The ion-exchanged process was performed for three times to obtain HY zeolite. Amorphous silica-alumina (ASA) was prepared as reported in our previous paper.[5] The mixture of HY zeolite and ASA (the weight ratio of 1 : 4) was used as the support of catalyst, which was extruded to form cylindrical shape. NiW/(ASA+HY) catalyst was prepared by using the incipient wetness method with aqueous solution of nickel nitrate hexahydrate and ammonium metatungstate, and settled at 25 °C for 12 h. After drying and calcination, NiW/(ASA+HY) catalyst was obtained, in which the concentration of NiO and WO_3 was 7.5 and 22.5 wt%, respectively. The catalysts with Y zeolite crystal size of 100, 300 and 500 nm were designated as Cat-1, Cat-2, Cat-3.

2.3 Characterizations

X-ray diffraction (XRD) analysis was used to identify the structure of synthesized samples, which was performed on a SIMADU XRD 6000 diffractometer with Cu Kα radiation (40 kV and 40 mA), and the XRD pattern was recorded in the 2θ range of 5 to 35°. While the SiO_2/Al_2O_3 ratio of Y zeolite was calculated on the basis of the unit cell parameters obtained from the position of [5 5 5] reflection peak by using Breck–Flanigen equation.[40] Fourier Transform Infrared (FT-IR) measurement was carried out on a MAGNAIR 560 instrument with the KBr technique to examine the framework vibration of samples. The morphology and crystal size of samples were studied with scanning electron microscopy (SEM) on a LEO435VP instrument. The crystal size distribution of synthesized Y zeolite was examined by a laser beam scattering technique on a S3500 instrument. N_2 adsorption–desorption analysis was carried out on a Micromeritics ASAP 2010 instrument at −196 °C in liquid nitrogen. The surface area of Y zeolite was calculated using the Brunauer–Emmett–Teller (BET) equation, and the total pore volume was obtained from the desorption branch of the isotherm at $P_i/P_o = 0.995$.

2.4 Catalyst assessment

The hydrocracking performance of catalyst was assessed in a fixed bed reactor using VGO as feedstock, the properties of VGO are shown in Table 1. Firstly, the catalyst was presulfurized using cyclohexane solution with 2 wt% CS_2 at 320 °C for 5 h, and then the hydrocracking assessment of catalyst was performed at 350 °C under H_2 pressure of 8 MPa with a H_2 to oil ratio of 1000 (v/v) and liquid hourly space velocity (LHSV) of 2.0 h^{-1}. After stabilization for 5 h, the reaction product was collected and analyzed by the simulated distillation (SIMDIS ASTMD-2887), which was fractionated into

Table 1 Properties of vacuum gas oil

Properties	
Density (20 °C) (g cm^{-3})	0.91
S content (μg g^{-1})	25
N content (μg g^{-1})	335
Boiling range (°C) IBP	
0.5%/10%	206/338
20%/30%	374/397
40%/50%	414/428
60%/70%	444/460
80%/90%	477/496
95%	517
FBP	573

naphtha (C_5–C_9, corresponding to <180 °C), middle distillates (C_{10}–C_{22}, corresponding to 180–350 °C), and residue product (C_{22+}, corresponding to above 350 °C) on the basis of boiling point distribution. The VGO conversion, the middle distillates yield and selectivity were calculated as follows:

$$\%C_{22+} \text{ conversion} = (\text{wt}\%C_{22+} \text{ in feed} - \text{wt}\%C_{22+} \text{ in product})/(\text{wt}\%C_{22+} \text{ in feed}) \times 100\%$$

$$\%(C_{10}\text{–}C_{22}) \text{ yield} = (\text{wt}\%(C_{10}\text{–}C_{22}) \text{ in product} - \text{wt}\%(C_{10}\text{–}C_{22}) \text{ in feed})/(\text{wt}\%C_{22+} \text{ in feed}) \times 100\%$$

$$\%(C_{10}\text{–}C_{22}) \text{ selectivity} = (\text{wt}\%(C_{10}\text{–}C_{22}) \text{ in product} - \text{wt}\%(C_{10}\text{–}C_{22}) \text{ in feed})/(\text{wt}\%C_{22+} \text{ in feed} - \text{wt}\%C_{22+} \text{ in product}) \times 100\%$$

3 Results and discussion

3.1 Synthesis of small crystal and high silica NaY zeolite

It has reported that seeding as structure directing agent plays an important role in the zeolite synthesis, adding seeding in the zeolite synthesis system can promote zeolite nucleation and growth. In this study, NaY zeolite was synthesized in the presence of seeding. Fig. 1 shows the XRD patterns of samples obtained with the seeding prepared with two kinds of silicon sources. Both samples exhibited the typical pattern of Y zeolite diffraction peaks (marked by "☆"), indicating that the synthesized sample was identified to be Y zeolite structure. FT-IR analysis can reflect the Si–O–Al linkages through the vibration band position to confirm the structure of zeolite. FT-IR spectra of synthesized samples are shown in Fig. 2. The IR band position and height of the two samples were nearly uniform. The peaks at 464, 1018 and 1139 cm^{-1} were attributed to the tetrahedral vibration of Y zeolite, the peaks at 713 and 787 cm^{-1} were related with the external linkage symmetrical stretching and the internal tetrahedral symmetrical stretching, and the peak at 578 cm^{-1} was assigned to double ring external linkage vibration associated with Y zeolite structure,[41–43] the FT-IR analysis result indicates that Y zeolite crystal was obtained, which was consistent with the XRD result.

SEM images of synthesized samples with seeding prepared with different silicon sources are shown in Fig. 3. The particles of NaY zeolite synthesized with seeding prepared with silica sol were nearly regular and not aggregated, and the sizes were about 100 nm. However, the regular and uniform particles of NaY zeolite synthesized with seeding prepared with sodium silicon were approximate 800 nm as shown in Fig. 3(b). Fig. 4 displays the particles sizes distribution of the synthesized NaY zeolite. For NaY zeolite synthesized with seeding prepared with silica sol, the particles sizes ranged from 60 to 155 nm, and the statistic average particles sizes was about 100 nm. But the particles sizes distribution was in the range of 670 to 910 nm, and the statistic average particles sizes was about 800 nm for NaY zeolite synthesized with seeding prepared with sodium silicon. The SiO_2/Al_2O_3 ratio of NaY zeolite, with seeding prepared with silica sol and sodium silicon, was 5.42 and 5.35, respectively.

It is concluded that silicon source, used to prepare seeding gel, had a strong effect on the crystal size of synthesized NaY zeolite, it may be that monopolymer silica species more easily released form silica sol than from sodium silicon tended to react with aluminum species to form nuclei precursor in the preparing seeding gel process.[44] Thus the presence of more

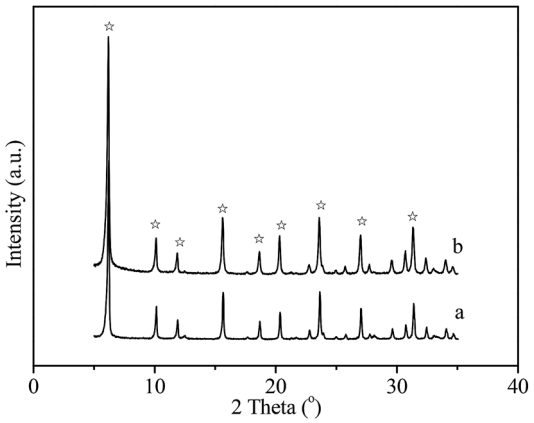

Fig. 1 XRD patterns of samples with seeding prepared with (a) silica sol and (b) sodium silicon.

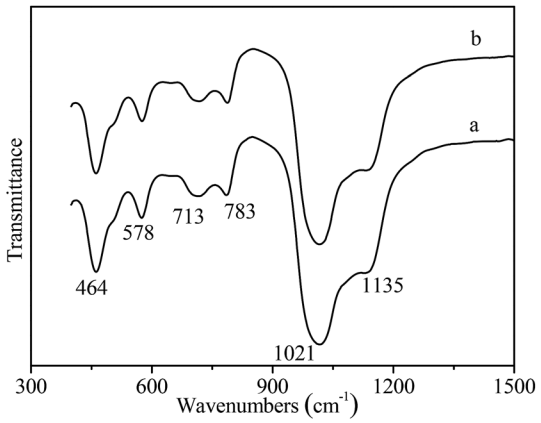

Fig. 2 FT-IR spectra of samples with seeding prepared with (a) silica sol and (b) sodium silicon.

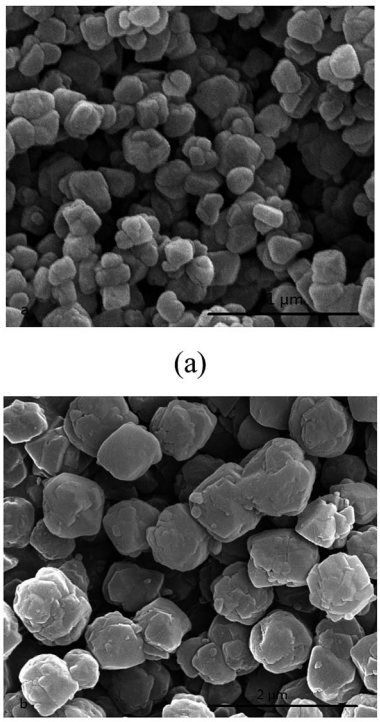

Fig. 3 SEM images of NaY zeolite synthesized with seeding prepared with (a) silica sol and (b) sodium silicon.

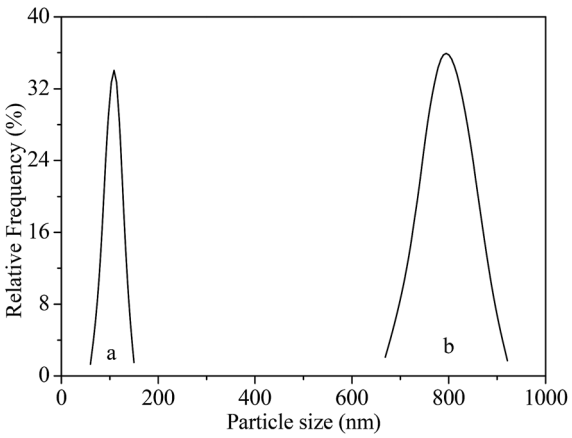

Fig. 4 Particles sizes distribution of NaY zeolite with seeding prepared with (a) silica sol and (b) sodium silicon.

nuclei precursor in seeding gel promoted more crystal nuclei formation, which was in favour of small crystal NaY zeolite formation.

3.2 Effect of aging time of seeding

Aging time affected the amount of nuclei formed in the seeding gel preparing process, and further controlled the crystal size of synthesized zeolite. The SEM images of synthesized NaY zeolite with seeding prepared at different aging time are shown in Fig. 5. The average crystal size of NaY zeolites was about 500 nm for the seeding gel aged for 6 h, when the aging time prolonged to 24 h, the crystal sizes of NaY zeolite decreased to about

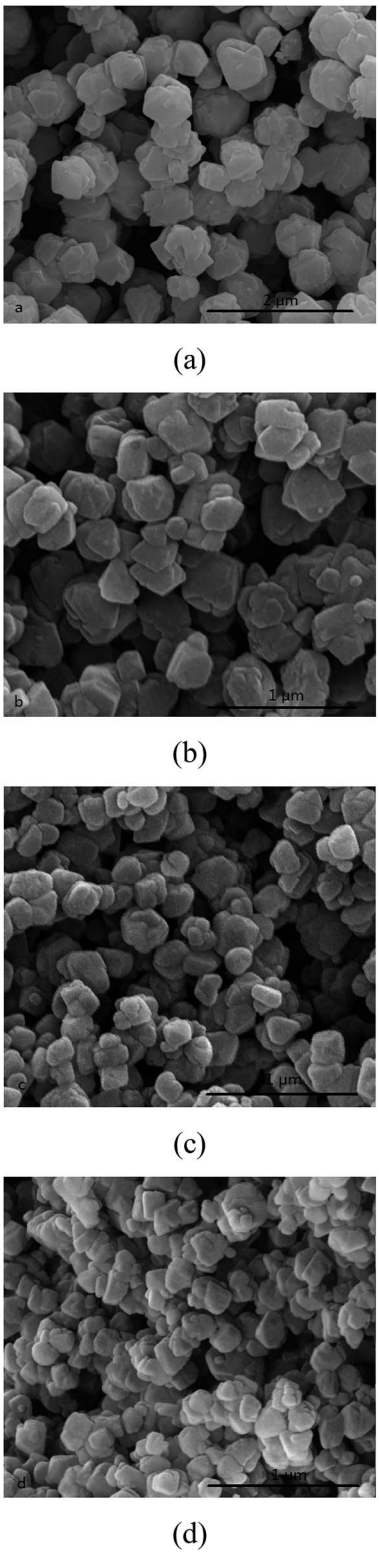

Fig. 5 SEM images of NaY zeolite with seeding prepared at different aging time (a) 6 h, (b) 12 h, (c) 24 h and (d) 36 h.

100 nm, but the crystal sizes had little change with the aging time further prolonging to 36 h. It indicates that the aging time of seeding was a crucial factor to regulate the crystal size of NaY zeolite, prolonging the aging time was beneficial to small crystal NaY zeolite formation due to more crystal nuclei formed in the seeding preparing process.

Fig. 6 shows the SiO_2/Al_2O_3 ratio of NaY zeolite with seeding prepared at different aging time. The SiO_2/Al_2O_3 ratio of NaY zeolite increased from 5.13 to 5.42 as the aging time of seeding extended from 6 to 24 h, but slightly decreased when the aging time prolonged to 36 h. It may be that the suitable aging time of seeding favored more silicon species inserting into nuclei, promoting the high SiO_2/Al_2O_3 ratio NaY zeolite formation. However, much longer aging time caused some silicon species dissolved from nuclei to slightly decrease the SiO_2/Al_2O_3 ratio of NaY zeolite.

3.3 Effect of the Na_2O content of seeding

Na_2O content for preparing seeding is also an important factor for the morphology of NaY zeolite. The SEM images of NaY zeolite with seeding prepared at the different molar ratios of Na_2O/Al_2O_3 (12, 14, 16 and 18) are shown in Fig. 7. Well-crystal NaY zeolite was obtained at the different Na_2O/SiO_2 ratios of seeding. When the Na_2O/Al_2O_3 molar ratio of seeding increased from 12 to 16, the crystal size of NaY zeolite exhibited a decrease trend, but the crystal size had no reduction as the Na_2O/Al_2O_3 molar ratio of seeding further increased. It is found that higher Na_2O content for preparing seeding favored the small crystal NaY zeolite synthesized, possibly due to more nuclei formation through high-polymerized silicon species depolymerizing into more low-polymerized silicon species in the high Na_2O content of preparing seeding system.

The SiO_2/Al_2O_3 ratios of NaY zeolite with seeding prepared at the different Na_2O/Al_2O_3 molar ratios are showed in Fig. 8. The SiO_2/Al_2O_3 ratio of NaY zeolite decreased with an increase of Na_2O/Al_2O_3 molar ratio in seeding, when the Na_2O/Al_2O_3 ratio was 12, the SiO_2/Al_2O_3 ratio of NaY zeolite reached to 5.54, but the SiO_2/Al_2O_3 ratio of NaY zeolite decreased to 5.27 as the Na_2O/Al_2O_3 ratio was up to 18. The lower SiO_2/Al_2O_3 ratio of NaY zeolite obtained at the higher Na_2O/Al_2O_3 ratio of seeding was ascribed to the existence of larger amount of low-polymerized

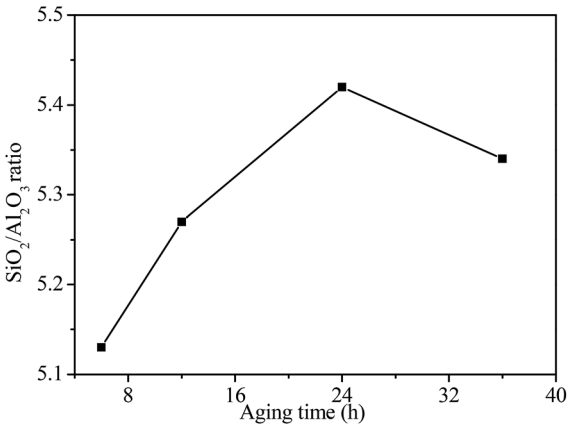

Fig. 6 SiO_2/Al_2O_3 ratios of NaY zeolite with seeding prepared at different aging time.

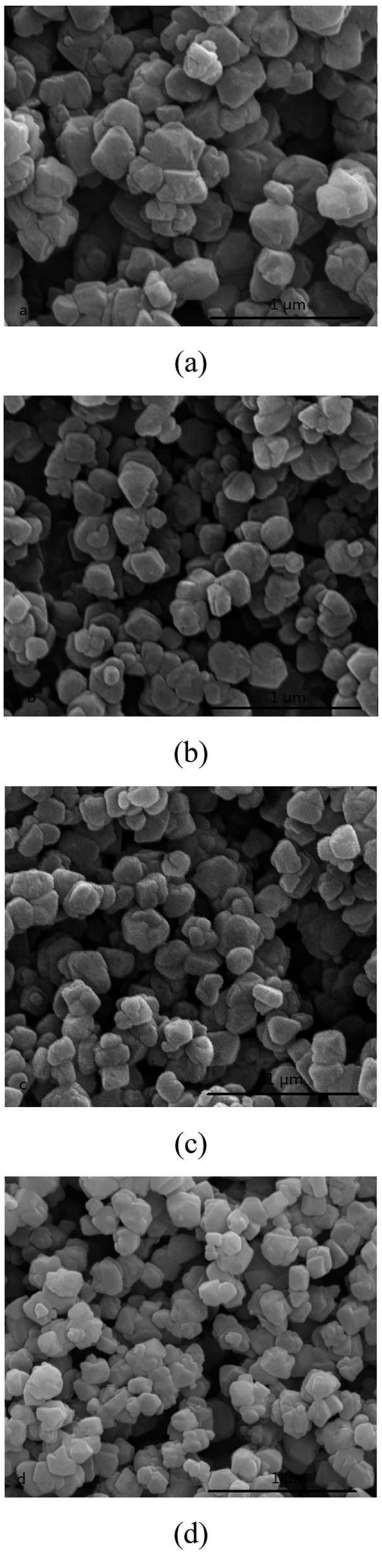

Fig. 7 SEM images of NaY zeolite with seeding prepared at $x$$Na_2O$: $1Al_2O_3$: 15 SiO_2 : 300H_2O: (a) $x = 12$, (b) $x = 14$, (c) $x = 16$ and (d) $x = 18$.

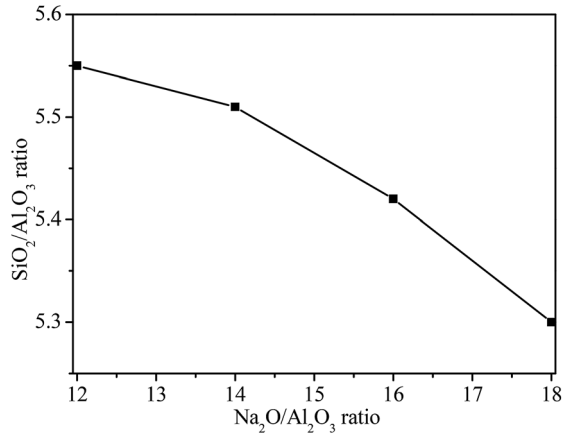

Fig. 8 SiO_2/Al_2O_3 ratios of synthesized NaY zeolite with seeding prepared at different Na_2O/Al_2O_3 ratios.

silicon species leading to less silicon species into the framework of NaY zeolite.

3.4 Texture properties

The N_2 adsorption–desorption isotherms of NaY zeolites with different crystal sizes are showed in Fig. 9. The NaY zeolite with crystal sizes of 300 and 500 nm gave typical type I isotherm, with filling of the micropore at low relative pressures ($P/P_0 < 0.1$). However, NaY zeolite with crystal size of 100 nm showed a hysteresis loop starting at $P/P_0 \approx 0.2$ and a steep nitrogen uptake at high relative pressure (0.9–1.0), corresponding to the type III isotherm,[45] which indicates that some mesopores and macropores were formed through the aggregation of small crystal to form the interparticle voids.[46] The surface area and pore structure of NaY zeolites with different crystal sizes are displayed in Table 2. Smaller crystal size NaY zeolite exhibited higher surface area, larger pore and mesoporous volumes. When the crystal size of NaY zeolite was 100 nm, the surface area reached to 728 $m^2\ g^{-1}$, and the pore volume and mesoporous volume was 0.4142 and 0.1228 ml g^{-1}, respectively, indicating that the reduction of crystal size of zeolite was beneficial to the enhancement of surface area and mesoporous volume, consistent with the report in the literatures.[8,10]

Table 2 Textural properties of the different crystal sizes NaY zeolites

Samples	S_{BET}[a] ($m^2\ g^{-1}$)	V_t[b] (ml g^{-1})	V_{meso}[c] (ml g^{-1})	D[d] (nm)
NaY-100	728	0.4142	0.1228	2.4
NaY-300	693	0.3891	0.0824	2.3
NaY-500	671	0.3718	0.0635	2.3

[a] S_{BET} is the BET specific surface area. [b] V_t is the total pore volume. [c] V_{meso} is the mesoporous volume. [d] D is the pore diameter.

3.5 Catalytic performances

Fig. 10 shows the hydrocracking conversions of VGO over all catalysts at reaction temperature of 350 °C. The VGO hydrocracking conversion was about 72.0% for Cat-1, but the conversion decreased to 61.0% for Cat-3, indicating that the VGO conversion over the corresponding catalyst decreased with an increase of the crystal size of Y zeolite. It may be that the small crystal zeolite with short pore channel and large mesoporous volume can reduce the diffusion limitation of large molecules, as well as larger amount of available acid sites were obtained on the larger surface area, which was favorable to the improvement of VGO hydrocracking reactivity.[47,48]

The yield and selectivity of middle distillates for all catalysts are shown in Fig. 11. Cat-1 had highest yield and selectivity of middle distillates in all catalysts, about 41.0 and 62.5%, respectively. The middle distillates yield and selectivity presented a decrease trend with an increase of the crystal size of Y zeolite, indicating that smaller crystal Y zeolite was beneficial to improve the middle distillates yield and selectivity in the hydrocracking process, possibly due to the higher dispersion of active metal species on larger surface area and the reduction of diffusion limitation of intermediate products through shorter pore channel and more mesoporous, which favored avoiding the overcracking of feedstock.

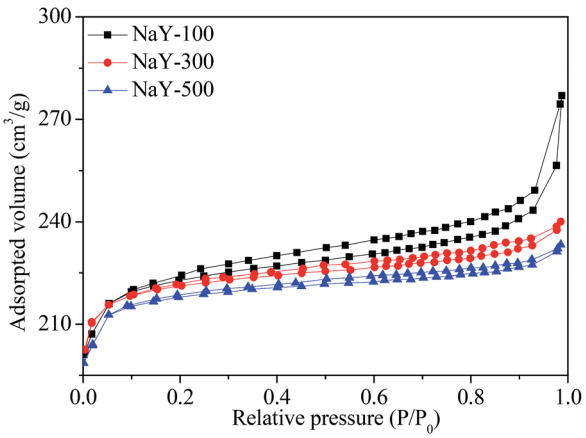

Fig. 9 N_2 adsorption–desorption isotherms of the different crystal sizes NaY zeolites.

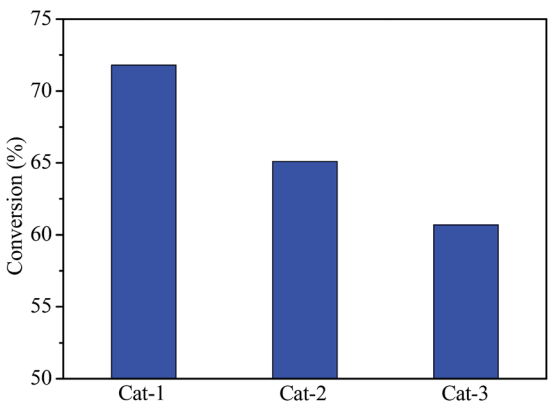

Fig. 10 VGO hydrocracking conversion over all catalysts at 350 °C.

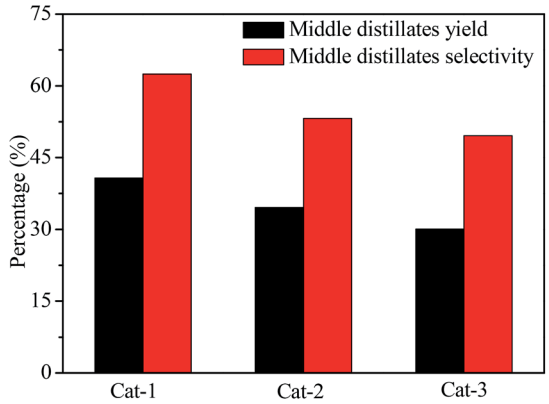

Fig. 11 Middle distillates yield and selectivity for all catalysts.

4 Conclusions

Small crystal NaY zeolite with high SiO_2/Al_2O_3 ratio was successfully synthesized with seeding, and the effects of silicon sources, aging time and Na_2O content of seeding on the crystal size and SiO_2/Al_2O_3 ratio of NaY zeolite was investigated. It is found that the silicon source for preparing seeding played an important role on the crystal size of the synthesized NaY zeolite, when silica sol was used to prepare seeding, NaY zeolite with the average size of 100 nm and SiO_2/Al_2O_3 ratio of 5.42 can be obtained, but NaY zeolite synthesized with seeding prepared with sodium silicon showed the average size of 800 nm and SiO_2/Al_2O_3 ratio of 5.35. Moreover, prolonging the aging time and increasing the Na_2O/Al_2O_3 ratio of seeding favored reducing the crystal size of NaY zeolite. In comparison of the hydrocracking performance of the catalyst containing different crystal sizes Y zeolite, Cat-1 catalyst had the VGO conversion of 72.0% and the middle distillates selectivity of 62.5% in the hydrocracking process, both were higher than those of other catalysts, indicating that the catalyst with small crystal Y zeolite presented perfect hydrocracking performance due to its especial properties.

Conflicts of interest

There are no conflicts to declare.

References

1 M. M. Robert and N. Y. Buffalo, *US Pat.* No. 2882244, 1959.
2 F. Delprato, L. Delmotte, J. L. Guth and L. Huve, *Zeolites*, 1990, **10**, 546–552.
3 T. Li, H. Y. Liu, Y. Fan, P. Yuan, G. Shi, X. T. Bi and X. J. Bao, *Green Chem.*, 2012, **14**, 3255–3259.
4 Y. C. Yin, L. H. Qin, X. F. Wang, G. G. Wang, J. Zhao, B. J. Liu and Y. Chen, *RSC Adv.*, 2016, **6**, 111291–111298.
5 Q. Y. Cui, Y. S. Zhou, Q. Wei, G. L. Yu and L. Zhu, *Fuel Process. Technol.*, 2013, **106**, 439–446.
6 W. Q. Jiao, W. H. Fu, X. M. Liang, Y. M. Wang and M. Y. He, *RSC Adv.*, 2014, **4**, 58596–58607.
7 W. W. Zhou, M. F. Liu, Q. Zhang, Q. Wei, S. J. Ding and Y. S. Zhou, *ACS Catal.*, 2017, **7**, 7665–7679.
8 L. Tosheva and V. P. Valtchev, *Chem. Mater.*, 2005, **17**, 2494–2513.
9 S. Elzey, A. Mubayi, S. C. Larsen and V. H. Grassian, *J. Mol. Catal. A: Chem.*, 2008, **285**, 48–57.
10 V. Valtchev and L. Tosheva, *Chem. Rev.*, 2013, **113**, 6734–6760.
11 L. Y. Hu, Z. K. Zhang and S. J. Xie, *Catal. Commun.*, 2009, **10**, 900–904.
12 R. P. L. Absil, A. Deptford and J. R. Katzer, *US Pat.* No. 5401704, 1995.
13 Q. Y. Cui, Y. S. Zhou, Q. Wei, X. J. Tao and G. L. Yu, *Energy Fuels*, 2012, **26**, 4664–4670.
14 S. F. Anis, G. Singaravel and R. Hashaikeh, *RSC Adv.*, 2018, **8**, 16703–16715.
15 Q. H. Li, D. Creaser and J. Sterte, *Chem. Mater.*, 2002, **14**, 1319–1324.
16 B. A. Holmberg, H. Wang, J. M. Norbeck and Y. Yan, *Microporous Mesoporous Mater.*, 2003, **59**, 13–28.
17 R. B. Benarmas, A. Bengueddach and F. D. Renzo, *Catal. Today*, 2014, **227**, 33–36.
18 P. Morales-Pacheco, F. Alvarez, L. Bucio and J. M. Dominguez, *J. Phys. Chem. C*, 2009, **113**, 2247–2255.
19 H. Wang, Z. Wang and Y. Yan, *Chem. Commun.*, 2000, 2333–2334.
20 O. Larlus, S. Mintova and T. Bein, *Microporous Mesoporous Mater.*, 2006, **96**, 405–412.
21 P. Morales-Pacheco, J. M. Domínguez, L. Bucio, F. Alvarez, U. Sedran and M. Falco, *Catal. Today*, 2011, **166**, 25–38.
22 H. Awala, J. P. Gilson, R. Retoux, P. Boullay, J. M. Goupil, V. Valtchev and S. Mintova, *Nat. Mater.*, 2015, **14**, 447–451.
23 S. Sang, Z. Liu, P. Tian, L. Qu and Y. Zhang, *Mater. Lett.*, 2006, **60**, 1131–1133.
24 M. Borel, M. Dodin, T. J. Daou, N. Bats, B. Harbuzaru and J. Patarin, *Cryst. Growth Des.*, 2017, **17**, 1173–1179.
25 H. M. Radman, A. A. Dabbawala, I. Ismail, Y. F. Alwahedi, S. Morin, M. Berthod and S. M. Alhassan, *Microporous Mesoporous Mater.*, 2019, **282**, 73–81.
26 D. Reinoso, M. Adrover and M. Pedernera, *Ultrason. Sonochem.*, 2018, **42**, 303–309.
27 T. F. Chaves, H. O. Pastore and D. Cardoso, *Microporous Mesoporous Mater.*, 2012, **161**, 67–75.
28 Y. S. Zhao, Z. Q. Liu, W. L. Li, H. H. Pa, Y. D. Liu, M. G. Li, L. J. Kong and M. Y. He, *Microporous Mesoporous Mater.*, 2013, **167**, 102–108.
29 M. I. Levinbuk, M. L. Pavlov and M. L. Kustov, *Appl. Catal., A*, 1998, **172**, 177–191.
30 B. A. Holmberg, H. T. Wang and Y. S. Yan, *Microporous Mesoporous Mater.*, 2004, **74**, 189–198.
31 S. Ferdov, K. Tsuchiya, N. Tsunoji and T. Sano, *Microporous Mesoporous Mater.*, 2019, **276**, 154–159.
32 P. Caullet, J. Hazm, J. L. Guth, J. F. Joly and F. Raatz, *Zeolites*, 1992, **12**, 240–250.
33 K. Suzuki and T. Hayakawa, *Microporous Mesoporous Mater.*, 2005, **77**, 131–137.

34 L. Chen, T. Xue, H. H. Wu and P. Wu, *RSC Adv.*, 2018, **8**, 2751–2758.
35 I. Mochida, S. Eguchi, M. Hironaka, S. Nagao, K. Sakanishi and D. Whitehurst, *Zeolites*, 1997, **18**, 142–151.
36 A. J. H. P. Poland and J. H. C. Hooff, *Appl. Catal., A*, 1992, **92**, 93–111.
37 B. W. Lu, T. Tsuda, Y. Oumi, K. Itabashi and T. Sano, *Microporous Mesoporous Mater.*, 2004, **76**, 1–7.
38 S. Gonthier and R. W. Thompson, *Studies in surface science and catalysis*, 1994, vol. 85, pp. 43–73.
39 P. K. Dutta and J. Bronic, *Zeolites*, 1994, **14**, 250–255.
40 D. W. Breck, *Zeolite molecular sieves: structure, chemistry, and use*, 1974, pp. 94–97.
41 J. C. Jansen, F. J. Van der Gaag and H. Van Bekkum, *Zeolites*, 1984, **4**, 369–372.
42 P. A. Jacobs, H. K. Beyer and J. Valyon, *Zeolites*, 1981, **1**, 161–168.
43 G. Coudurier, C. Naccache and J. C. Vedrine, *J. Chem. Soc., Chem. Commun.*, 1982, **24**, 1413–1421.
44 R. F. Di, A. Albizane and M. Nicolle, *Stud. Surf. Sci. Catal.*, 1991, **65**, 603–612.
45 M. Kruk and M. Jaroniec, *Chem. Mater.*, 2001, **13**, 3169–3183.
46 B. Z. Zhan, M. A. White and M. Lumsden, *Chem. Mater.*, 2002, **14**, 3636–3642.
47 M. Firoozi, M. Baghalha and M. Asadi, *Catal. Commun.*, 2009, **10**, 1582–1585.
48 M. A. Camblor, A. Corma and A. Martinez, *J. Catal.*, 1998, **179**, 537–547.